Striations in dual-frequency capacitively coupled CF_4 plasmas

Y.-X. Liu,[1] I. Korolov,[2] E. Schüngel,[3] Y.-N. Wang,[1] Z. Donkó,[4] and J. Schulze[2,5]

[1]*Key Laboratory of Materials Modification by Laser, Ion, and Electron Beams (Ministry of Education), School of Physics, Dalian University of Technology, Dalian 116024, China*
[2]*Institute for Electrical Engineering, Ruhr-University Bochum, 44801 Bochum, Germany*
[3]*Evatec AG, CH-9477 Trübbach, Switzerland*
[4]*Institute for Solid State Physics and Optics, Wigner Research Centre for Physics, Hungarian Academy of Sciences, Konkoly-Thege Miklós str. 29-33, H-1121 Budapest, Hungary*
[5]*Department of Physics, West Virginia University, Morgantown, West Virginia 26506-6315, USA*

Abstract: Striations in dual-frequency (DF, 8/40 MHz) capacitively coupled CF_4 plasmas have been investigated by phase resolved optical emission spectroscopy and via particle in cell/Monte Carlo collision simulations. The properties of striated structures of various plasma parameters in a DF discharge and the effect of the high-frequency voltage amplitude on the striated structures and charged species densities were studied.

Keywords: Striations, phase resolved optical emission spectroscopy, PIC/MCC simulations, electronegative capacitive coupled plasmas

1. General

Capacitively coupled radio-frequency (CCRF) discharges operated in electronegative gases, such as O_2 CF_4, SF_6, etc., have been widely used in material processing industries, for thin film deposition, dielectric etching, etc [1]. Previously, we observed the self-organized striated structures of the plasma emission in single-frequency (SF) capacitively coupled CF_4 plasmas via phase resolved optical emission spectroscopy (PROES) and their formation has been analyzed by Particle in Cell / Monte Carlo collision (PIC/MCC) simulations [2-4]. The effects of the external control parameters, such as the driving frequency, pressure, rf voltage, have been studied, and a phase diagram as a function of the pressure and voltage amplitude was established to present the parametric window for the presence of the striations. It was found that the striations are generally present at higher pressures and/or rf voltages, where the ion density exceeds a "critical value" so that they can respond to the rf electric field inside the plasma bulk. This leads to the generation of space charge, wherever ion density gradients are present. These space charges cause a striated profile of the electric field and, thus, the ionization/excitation. It should be noted that all the work mentioned above has been done in SF CCRF discharges [2-4].

In this work, we extend this topic to dual frequency (DF, 8/40 MHz) discharges under the same conditions as in the SF case (ϕ_L = 300 V, p =100 Pa, L=1.5 cm).

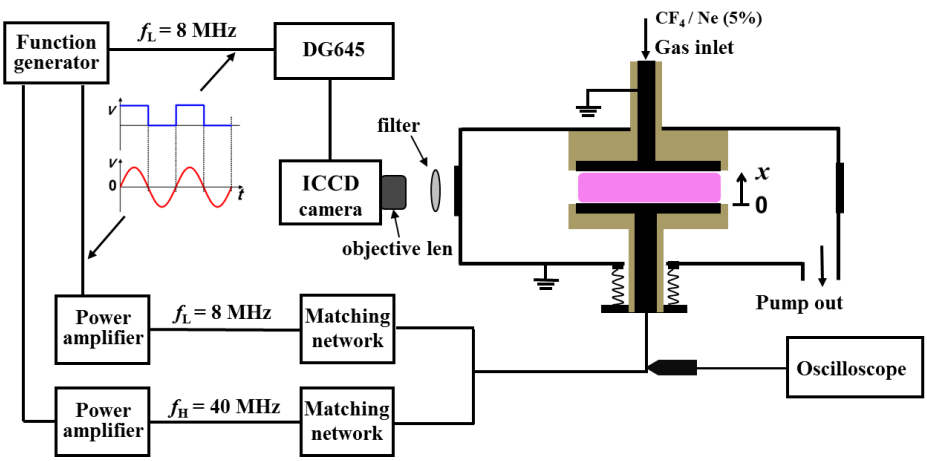

Fig. 1 Schematic of the DF CCRF plasma reactor chamber, supplemented with a phase resolved optical emission spectroscopy diagnostic system.

2. Experiment and PIC/MCC simulations

The plasma reactor together with the diagnostic tools is schematically shown in Fig. 1. The plasma is produced in CF_4 with a 5% admixture of Ne as a probe gas for PROES, between two parallel circular stainless-steel electrodes. Both electrodes are 10 cm in diameter, separated by 1.5 cm. A two-channel function generator is used to generate two sinusoidal signals (8 MHz / 40 MHz) with a locked phase (φ = 0 °), and then these two signals are amplified by two power amplifiers and then applied to the lower electrode via two matching networks. The upper electrode and the chamber wall are grounded. A high-voltage probe (Tek P6015A) connected to a digital oscilloscope is used to monitor the voltage waveforms at the powered electrode. The working pressure is fixed at 100 Pa, the LF voltage amplitude at 300 V, and the HF voltage amplitude is adjusted in the range of 0 V ~ 160 V.

An ICCD camera (Andor iStar DH734) equipped with an objective lens is used to detect the light emission from the plasma. An interference filter is used to select the emission line at 585.5 nm, corresponding to the $2p_1 \rightarrow 1s_2$ Ne transition. The camera gate is controlled in a synchronized manner by a pulse delay generator, which is triggered by a square signal with the low frequency (8 MHz) provided by the function generator. From the light emission measurements, that are performed in a sequence through all times of the LF period (~ 125 ns), the spatio-temporal distribution of the electron-impact excitation rate from the ground state into $Ne2p_1$-state is calculated based on a collisional-radiative model (for more details see [5,6]).

Our numerical studies are based on a bounded 1D3V Particle in Cell simulation code, complemented with a Monte Carlo type treatment of collision processes (PIC/MCC), see [7]. For a comparative study between experiment and simulation, in all cases the HF and LF amplitudes of the measured voltage waveforms are used as input for the PIC/MCC simulations.

3. Results

Figure 2(a) shows the PROES result for the spatio-temporal plot of the electron-impact excitation rate from the ground state into $Ne2p_1$–state. One can see that at each electrode excitation maxima occur at three distinct times (indicated by the three white arrows) within each half of the LF period, due to the modulation of the HF source. Particularly, the measured excitation rate exhibits

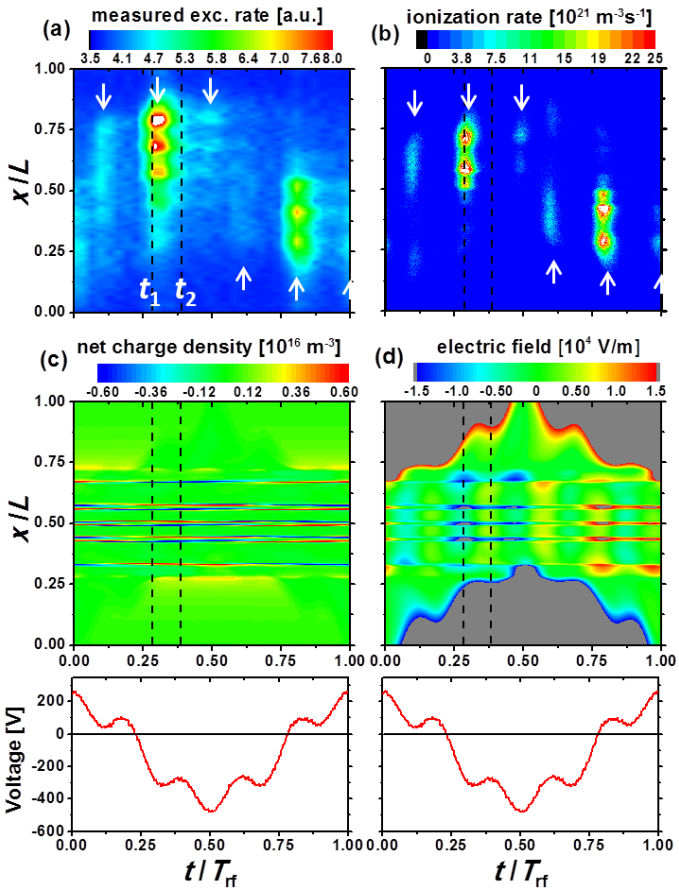

Fig. 2 PROES results: spatio-temporal plot of the electron-impact excitation rate from the ground state into $Ne2p_1$-state (a). PIC/MCC simulation results: spatio-temporal plots of the electron-impact ionization rate (b), net charge density (c), electric field (d). The bottom panels show the DF voltage waveform. Conditions: f_L = 8 MHz, f_H = 40 MHz, ϕ_L = 300 V, ϕ_H = 80 V and p = 100 Pa.

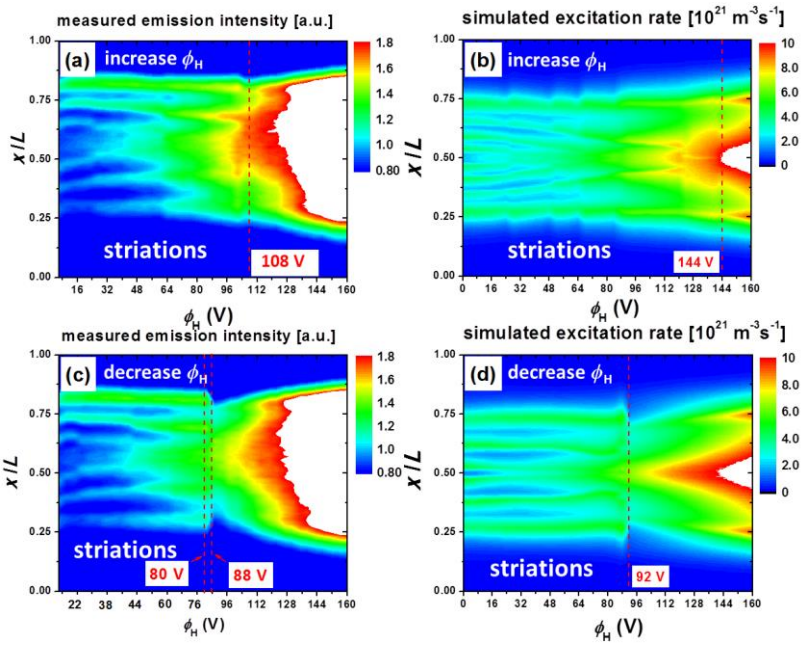

Fig. 3 Evolution of the axial distribution of the measured emission intensity (a and c) and simulated electronic excitation rate (b and d) as a function of ϕ_H. The other conditions are the same as in Fig. 2.

its maximum (or is constructively enhanced) when the oscillation of the HF and LF sheaths is in phase (i.e., the HF and LF sheaths are expanding or collapsing at the same time), while it is nearly invisible, when the motion of the HF and LF sheaths is out of phase. These experimentally observed patterns are in good qualitative agreement with the striated spatio-temporal distribution of the ionization/excitation rate obtained from the simulations. The spatially modulated excitation/ionization rate is caused by the spatially modulated electric field profile (see Fig. 2d).

In both the experiment and the simulation, we observe a hysteresis of the axial distributions of the emission intensity and the electron excitation rate when increasing and decreasing ϕ_H at an increment of 4 V. We see that by increasing ϕ_H to 160V in the simulation (see left column of Fig.3), the striations disappear at 108 V. In contrast, the mode transition point occurs at 88 V, when decreasing ϕ_H. This is clearly a hysteresis, which can also be observed in PIC/MCC simulations (see the right column of Fig.3).

Fig. 4 shows the CF_3^+ ion density as a function of the ϕ_H. The peak density exhibits a "sawtooth-like" increase with increasing ϕ_H, i.e., a density drop occurs whenever one central density peak is missing. At $\phi_H \geqslant 144$ V, there is only one density peak left inside the bulk. With the increase of ϕ_H, the striations widen, leading to a decrease of the number of the ion density peaks, shown by the numbers in Fig. 4. By decreasing ϕ_H, the ion density maximum decreases monotonously, with a density jump occuring at 92 V. This leads to a hysteresis loop in the CF_3^+ ion density maximum. However, the CF_3^+ ion density minimum inside the bulk region is almost independent of ϕ_H, regardless of whether ϕ_H is increased or decreased, as the ion density minimum inside the bulk region is primarily determined by the LF frequency [3, 4]. The spatially averaged electron density increases with ϕ_H in a similar way as the CF_3^+ ion density maximum, with the exception that an electron density jump occurs, whenever one central density peak vanishes. When decreasing ϕ_H, the electron density exhibits the same dependence on ϕ_H as the CF_3^+ ion density maximum. Please note that the maximum and minimum of the F^- ion density as functions of ϕ_H are not shown here, because they change with ϕ_H in a very similar manner compared to the maximum and minimum of the CF_3^+ ion density.

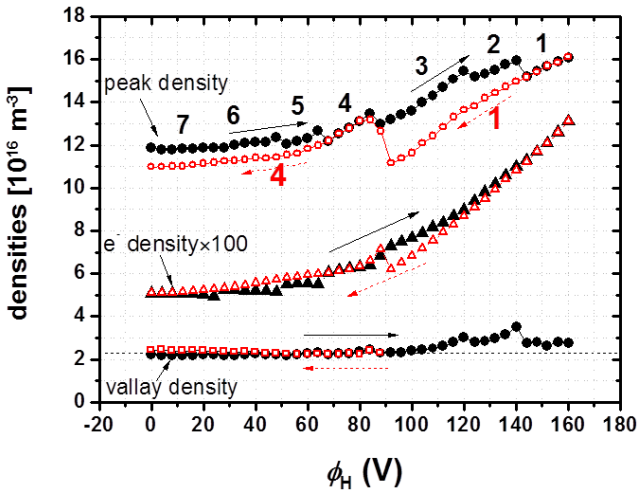

Fig. 4 Simulation results: the maximum and minimum of the CF_3^+ ion density and the spatially averaged electron density (multiplied by a factor of 100) as a function of ϕ_H. Thee number of the ion density peaks inside the bulk region is indicated by the labels. The conditions are the same as in figure 2.

4. Conlusions

Striations in dual-frequency (DF, 8/40 MHz) capacitively coupled CF_4 plasmas at 100 Pa have been investigated by PROES and via PIC/MCC simulations. The properties of striated structures of various plasma parameters in a DF discharge and the effect of the HF voltage amplitude ϕ_H on the striated structures and charged species densities were studied. The measured spatiotemporal electronic excitation rates at different ϕ_H are in good agreement with the simulation results. It was found that the excitation/ionization patterns are modulated not only in space, but also in time by two frequencies.

As ϕ_H increases, the width of the ion density peaks, generally increases, leading to a decrease of the number of striations and finally to the disappearance of striations at higher ϕ_H. The width of each single ion density peak is believed to be determined by a local balance between the ion generation (via electron-impact ionization and dissociative attachment) and losses (primarily via recombination of the positive and negative ions, and detachment) for a single ion density peak. Particularly, we observed a hysteresis of the axial profiles of the measured plasma emission intensity and the simulated electron-impact excitation rate induced by increasing and decreasing ϕ_H continuously.

The dependence of the width of each single ion density peak on ϕ_H was found to play a key role for the appearance of the hysteresis. When increasing ϕ_H, each ion density peak gradually widens, and in the meantime the ion density peaks vanish one after another until one density peak is left inside the bulk region. In contrast, when decreasing ϕ_H from 160 V the unimodal ion density profile is narrowing linearly, until at ϕ_H = 92 V the unimodal ion density profile becomes unstable and then it collapses flashily, leading to the formation of a four-peak profile at ϕ_H =88 V.

5. Acknowledgments

This work has been financially supported by the National Natural Science Foundation of China (NSFC) (Grant Nos. 11875100, and 11722541), by the Hungarian National Research, Development and Innovation Office, via Grant No. NKFIH 119357, by the German Research Foundation (DFG) within the frame of the collaborative research center SFBTR87 (project C1), and by the U.S. National Science Foundation (Grant No. 1601080).

6. References

[1] Lieberman M A and Lichtenberg A J 2005 Principles of Plasma Discharges and Materials Processing 2nd edn (Hoboken, NJ: Wiley Interscience).

[2] Y.-X. Liu, E. Schüngel, I. Korolov, Z. Donkó, Y.-N. Wang and J. Schulze, Phys. Rev. Lett. **116** 255002 (2016)

[3] Y.-X. Liu, I. Korolov, E. Schüngel, Y.-N. Wang, Z. Donkó and J. Schulze, Plasma Sources Sci. Technol. **26** 055024 (2017)

[4] Y.-X. Liu, I. Korolov, E. Schüngel, Y.-N. Wang, Z. Donkó and J. Schulze, Phys. Plasmas **24** 073512 (2017)

[5] T. Gans, D. O' Connell, V. Schulz-von der Gathen and J, Waskoenig, Plasma Sources Sci. Technol. **19** 034010 (2010)

[6] J. Schulze, E. Schüngel, Z. Donkó, D. Luggenhölscher and U. Czarnetzki, J. Phys. D: Appl. Phys. **43** 124016 (2010)

[7] Z. Donkó, Plasma Sources Plasma Sources Sci. Technol. **20** 024001 (2011)